Residual Ca^{2+} channel current modulation by megestrol acetate via a G-protein α_S-subunit in rat hypothalamic neurones

Anna-Maria N. Costa, Katherine T. Spence, Carlos R. Plata-Salamán * and Jarlath M. H. ffrench-Mullen†

*Department of Pharmacology, Zeneca Pharmaceuticals, Zeneca Inc., Wilmington, DE 19850-5437 and *School of Life and Health Sciences, University of Delaware, Newark, DE 19716, USA*

1. The inhibition of voltage-activated Ca^{2+} channel currents by the orally active progesterone derivative, megestrol acetate (MA), was examined in freshly dissociated rat ventromedial hypothalamic nucleus (VMN) neurones using the whole-cell voltage-clamp technique with 10 mM Ba^{2+} as the charge carrier.

2. The steady-state inhibition of the peak high-threshold Ca^{2+} channel current evoked by depolarization from −80 to −10 mV by MA increased in a concentration-dependent fashion. MA inhibited a fraction of the whole-cell Ca^{2+} channel current while progesterone had no effect on the peak Ca^{2+} channel current (7% at 10 μM). The low-threshold Ca^{2+} (T-type) current, evoked from −100 to −30 mV, was unaffected by MA.

3. Intracellular dialysis with MA had no effect on the Ca^{2+} channel current. Concomitant extracellular perfusion of MA showed normal inhibitory activity, suggesting that the MA binding site can only be accessed extracellularly.

4. The high-threshold Ca^{2+} channel current in VMN neurones was found to consist of four pharmacologically distinguishable components: an N-type current, an L-type current, a P-type current, and a residual current. MA had no effect on the N-, L- and P-type Ca^{2+} channel currents, but inhibited the residual current.

5. In neurones isolated from cholera toxin-treated animals, the MA-induced inhibition of the Ca^{2+} channel current was significantly diminished, suggesting a G-protein α_s-subunit involvement.

6. Treatment with antisense phosphothio-oligodeoxynucleotides to the $G\alpha_s$-subunit (antisense-$G\alpha_s$) significantly reduced the MA-induced inhibition of the Ca^{2+} channel current. Treatment with either sense-$G\alpha_s$ or antisense-$G\alpha_{11}$ had no effect, confirming a $G\alpha_S$-subunit involvement.

7. These results suggest that appetite enhancement induced by MA in cachectic patients may in part be due to a novel central nervous system action, that is, inhibition of a fraction of the whole-cell Ca^{2+} channel current to attenuate the firing of VMN neurones that may be involved in satiety mechanisms.

The hypothalamus is well established as an integrative centre for a number of behavioural and homeostatic activities, including both feeding and reproductive behaviours. Physiological and clinical evidence from human and animal studies has indicated the involvement of the hypothalamic ventromedial nucleus (VMN) in the regulation of food intake. Bilateral lesions or tumours of the VMN have been shown to induce hyperphagia and obesity in various species, including humans (for review, see Plata-Salamán, 1991). In contrast, repeated or chronic electrical stimulation of the VMN results in a decreased weight gain in normophagic animals (Bielajew, Stenger & Schindler, 1994). Thus, the VMN has been associated with the suppression of food intake.

Cachexia, common in a substantial proportion of cancer patients and during other chronic diseases including AIDS,

† To whom correspondence should be addressed.

is associated with appetite suppression (Tisdale, 1993). This leads to weight loss, physical wasting and malnutrition, which impairs the quality of life and may also lead to a poor prognosis in terms of cancer treatment (Loprinzi, Goldberg & Burnham, 1992). The current pharmacological management of cachexia includes the use of a variety of steroids (Loprinzi *et al.* 1992; Bruera, 1992). Megestrol acetate (MA; 17α-acetoxy-6-methyl-4,6-pregnadiene-3,20-dione) is a synthetic, orally active progestogen used for the treatment of patients with metastatic breast and endometrial cancer (Gregory, Cohen, Oines & Mims, 1985; Morgan, 1985). It was found to stimulate appetite and cause weight gain (Aisner, Tchekmedyian, Moody & Tait, 1987). Several clinical trials have established that MA causes appetite stimulation and weight gain with few side-effects in cancer or AIDS patients with anorexia/cachexia (Graham, Mikolich, Fisher, Posner & Dudley, 1994: Nelson, Walsh & Sheehan, 1994). The weight gain resulting from MA treatment is due to an increase in adipose tissue, hence an increase in body mass (Loprinzi, Schaid, Dose, Burnham & Jensen, 1993). However, the mechanism by which MA stimulates feeding and weight gain is unknown.

The Ca^{2+} influx through voltage-gated Ca^{2+} channels has a vital role in the control of neurotransmitter release and membrane excitability. The modulation of Ca^{2+} channels controls the extent of Ca^{2+} entry and thus provides a way of regulating neuronal function. Multiple classes of voltage-dependent Ca^{2+} channels exist in both peripheral and central mammalian neurones: the low-threshold T-type and the high-threshold N-type (ω-conotoxin GVI-sensitive), L-type (dihydropyridine-sensitive), P-type (ω-agatoxin IVA-sensitive) channels and a residual-type (resistant to these antagonists) channel (see Tsien, Lipscombe, Madison, Bley & Fox, 1988; Regan, Sah & Bean, 1991; Mintz, Adams & Bean, 1992).

Given that certain steroids inhibit voltage-gated Ca^{2+} channel currents (ffrench-Mullen, Danks & Spence, 1994*a*) and that MA stimulates food intake, we therefore examined whether MA would have an inhibitory effect on Ca^{2+} channel currents in the VMN. We report here that in freshly isolated VMN neurones, MA reversibly inhibits a fraction of the voltage-gated Ca^{2+} current that is insensitive to blockers of the N-, L- and P-type Ca^{2+} channel currents. This inhibition of the residual Ca^{2+} channel current is modulated through the G-protein α_S-subunit. These results suggest that a possible mode of action of MA is to reduce the firing tone of VMN neurones, which may be expressed as the promotion of feeding.

METHODS

Implantation of brain cannulas and osmotic minipumps

Brain cannulas and osmotic minipumps were implanted as previously described in detail (ffrench-Mullen *et al.* 1994*a*). Rats were allowed to recover for 7–10 days after surgery before osmotic minipump implantation. Alzet osmotic minipumps (Alza Corporation, Palo Alto, CA, USA) were used to accomplish the continuous intracerebroventricular microinfusion of pertussis toxin (1000 ng (24 h)$^{-1}$ for 48 h), cholera toxin (100 ng (24 h)$^{-1}$ for 48 h) and the sense and antisense phosphothio-oligodeoxynucleotides (15 μg (24 h)$^{-1}$ for 48 h). The nominal pumping rate of the osmotic minipumps is 1 μl h^{-1} (7 days)$^{-1}$ (Model 2001). For minipump implantation, rats were anaesthetized with sodium pentobarbitone (65 mg kg^{-1} I.P.). The filled minipump was connected, by a short polyethylene tube (1·1 mm i.d.), to an insert cannula of 29-gauge stainless-steel tubing, L-shaped so that when inserted into the guide cannula its terminal end just reached the tip of the guide cannula. The minipump was inserted into the subcutaneous interscapular space, and the L-shaped steel tubing was cemented in place with dental acrylic.

Cell preparation and whole-cell patch-clamp recording

Rats (100–200 g body weight; Hilltop Laboratories, Scotsdale, PA, USA) were anaesthetized with 100% CO_2, decapitated, and their brains rapidly removed. Coronal slices (400 μm thick) of the hypothalamus were cut using a Vibratome (Oxford Instruments). The slices were equilibrated for 1 h in artificial cerebrospinal fluid (ACSF) at 37 °C and aerated with 95% O_2–5% CO_2. The ACSF contained (mM): NaCl, 126; KCl, 2·5; NaH_2PO_4, 1·24; $CaCl_2$, 2·4; $MgCl_2$, 1·3; $NaHCO_3$, 26; D-glucose, 10 (pH 7·4). Following this, the slices were then incubated with trypsin Type XI (2 mg ml^{-1}) and collagenase type A (1 mg ml^{-1}) for 60 min. The slices were then rinsed three times with enzyme-free ACSF at room temperature, then transferred to a different chamber containing enzyme-free ACSF and trypsin inhibitor (Type 2S; 1 mg ml^{-1}), and maintained at 30 °C. The ventromedial nucleus of the hypothalamus (VMN) was then punched out with a micro-punch, mechanically dissociated by trituration and plated for subsequent recording as previously described (ffrench-Mullen *et al.* 1994*a*).

Macroscopic whole-cell Ca^{2+} channel currents were recorded at room temperature (22–25 °C) using 10 mM Ba^{2+} as the external charge-carrying divalent cation, and with the Ca^{2+} chelator Cs_4-BAPTA (Molecular Probes) in the intracellular solution to reduce Ca^{2+}-promoted Ca^{2+} channel inactivation. The bath solution contained (mM): $BaCl_2$, 10; TEA-Cl, 15; $MgCl_2$, 1; $CsCl_2$, 5; 4-aminopyridine, 5; Hepes, 10; Trizma base, 120; and glucose, 25. Tetrodotoxin (2 μM) was added to the bath solution to block voltage-dependent Na^+ channels; the solution was adjusted to a pH of 7·4 with methanesulphonic acid, and to an osmolality of 320 mosmol (kg H_2O)$^{-1}$. The pipette solution contained (mM): Trizma base, 130; Hepes, 10; Cs_4-BAPTA, 10; leupeptin, 0·1; and ATP–Tris, 5. The ATP regeneration system, Tris–phosphocreatinine (20 mM) and creatine kinase (20 U ml^{-1}), was added to the internal solution to minimize run-down of the Ca^{2+} currents. The internal solution was adjusted to pH 7·3 with methanesulphonic acid and to an osmolality of 315 mosmol (kg H_2O)$^{-1}$. The rate of run-down under these conditions was $< 5\%$ over a 30 min period. Recordings were carried out using the whole-cell patch-clamp technique as previously described (ffrench-Mullen *et al.* 1994*a*). Evoked currents were filtered at 10 kHz (−3 dB, 8-pole low pass Bessel filter), digitally sampled at 500 μs per point (50 μs per point for tail current measurements), and stored on magnetic media in digital form for later analysis. Capacitative and leakage currents were digitally subtracted (P/N; subtraction of an average of four appropriately scaled current responses to a 10 mV hyperpolarizing voltage step) on-line from all records using pCLAMP 5.51 (Axon Instruments). A rapid superfusion system consisting of a side-by-side array of six 200 μm i.d. capillary tubing was positioned within approximately

500 μm of the cell under study. Drug solutions were applied by gravity feed and flow was computer controlled via solenoid valves (BME Systems, Baltimore, MD, USA). Solution changes were accomplished within 300–500 ms. In order to examine the inhibition of the peak current, and the respective types of Ca^{2+} currents, Ca^{2+} channel currents were typically evoked by 200 ms voltage steps to −10 mV from a holding potential of −80 mV at 40 s intervals. To examine the current–voltage relationships and tail currents, 50 ms voltage steps (evoked at 20 s intervals) were generated.

Data analysis

For the quantification of inhibition, peak current values were used. Percentage inhibition was determined according to the formula $100(1 - I_{drug}/I_{control})$, where $I_{control}$ is the leak-subtracted peak current amplitude prior to the drug application and I_{drug} is the peak current amplitude in the presence of the test drug. During the drug applications, the Ca^{2+} channel current was examined using the 200 ms duration depolarizing step protocols. The I_{drug} value used in the calculation of percentage block was obtained after being at a steady-state value for 1 min. Concentration–effect data were fitted with a non-linear least-squares program (NFIT, Island Products, Galveston, TX, USA) according to the logistical equation $B = 100/1 + (IC_{50}/[D])^{n_H}$ where [D] is the drug concentration, IC_{50} is the concentration resulting in 50% block, and n_H is an empirical parameter that describes the steepness of the curve and has the same meaning as the Hill coefficient. Tail current amplitudes were estimated by fitting the falling phase of the current to a single exponential and extrapolating the curve to zero time. Activation curves were determined by plotting the tail current amplitudes at −80 mV following activation of the current by test pulses to different voltages, and were fitted to a Boltzmann equation $\{1 + \exp[(V_{½} - V)/k]\}^{-1}$, where $V_{½}$ is the voltage for half-maximal activation and k is the slope factor; fitting was done by NFIT. All traces are the mean of three steps and are leak subtracted; current–voltage (I–V) data points at each potential are connected by a cubic spline in SigmaPlot Windows V1 (Jandel Scientific, San Rafael, CA, USA). Final plotting was performed with SigmaPlot. All quantitative data are expressed as means ± S.E.M.; n indicates the number of cells examined. Statistical analysis was performed using the paired or unpaired Student's t test, or the Mann–Whitney test, depending upon the characteristics of the data. Results were considered significant only for $P < 0.05$.

Materials

All chemicals used in this study, except where noted, were obtained from Sigma and included the following: megestrol acetate, medroxyprogesterone acetate, medroxyprogesterone, progesterone, nifedipine, trypsin XI, the 20 amino acid protein kinase A inhibitor (rabbit sequence), pertussis toxin (PTX) and guanosine 5′-*O*-(2-thiodiphosphate) (GDP-β-S). Collagenase type A (Boehringer Mannheim, Indianapolis, IN, USA), ω-conotoxin GVIA (CgTX) (Peninsula Laboratories, Belmont, CA, USA); ω-agatoxin IVA (Aga IVA) (Peptide Institute Inc., Osaka, Japan); Rp-cyclic adenosine 3′,5′-monophosphothioate (Rp-cAMPS), 3-[1-(3-dimethylaminopropyl)-indol-3-yl]-3-(indol-3-yl)-maleimide or bisindolylmaleimide (BIS) (Calbiochem, San Diego, CA, USA); and PKCI(19–36) pseudosubstrate inhibitor (Bachem Bioscience, Inc., Philadelphia, PA, USA). Stock solutions (10 mM) of the steroid in ethanol were prepared daily; with steroid concentrations of 100 μM, final ethanol volume never exceeded 0·1% and the latter concentration has no effect on the Ca^{2+} channel current. Stock solutions (10 mM) of nifedipine and ω-conotoxin were prepared weekly in ethanol and H_2O, respectively. Oligodeoxynucleotides (18 and 20 bases) were thiolated at all positions and were synthesized by the DNA Analysis Facility of The Johns Hopkins University. Numbers refer to the first base of the sequence to which the primer corresponds relative to the adenine of the initiating ATG. Antisense-Gα_{11} 605, 5′-GGTGGGCAGGTAGCCTAC-3′ was taken from ffrench-Mullen, Plata-Salamán, Buckley & Danks (1994*b*); antisense-Gα_s, 5′-CATGGCGGCGGCGGGGCGCG-3′ and sense-Gα_s, 5′-CGCGCCCCGCCGCCGCCATG-3′ were taken from Wang, Watkins & Malbon (1992).

RESULTS

The data presented in this report represent the results of whole-cell recordings of Ca^{2+} channel currents from more than 160 neurones acutely dissociated from the rat ventromedial hypothalamic nucleus (VMN). Macroscopic voltage-gated Ca^{2+} channel currents were recorded using 10 mM Ba^{2+} as the external charge-carrying cation.

Inhibition of the Ca^{2+} channel current

From a holding potential of −80 mV, depolarizing voltage steps to potentials positive to −60 mV elicited a high-threshold inward Ca^{2+} channel current that peaked rapidly, and decayed gradually with maintained depolarizations of 200 ms (Fig. 1*A*). Superfusion with 50 μM Cd^{2+} virtually eliminated the inward current (98 ± 3% block, $n = 6$; not shown), demonstrating that it is carried by Ca^{2+} channels. Peak Ca^{2+} channel current was reversibly reduced in a concentration-dependent fashion by megestrol acetate (MA), beginning with concentrations as low as 10 pM.

As illustrated in Fig. 1*A*, increasing concentrations of MA inhibited the peak Ca^{2+} channel current by 9, 17 and 26% at 10 pM, 10 nM and 10 μM, respectively. In this neurone, inhibition was reversed to 92% of control with a wash in drug-free solution.

A low-threshold and transient Ca^{2+} channel current (T-type) was evoked with depolarizing voltage steps (100 ms) from −100 mV to −20 mV, with a maximal amplitude at −30 mV, as previously reported (Akaike, Kostyuk & Osipchuk, 1989). Perfusion with MA (10 pM–10 μM) had no effect on this current ($n = 5$; not shown).

The time course of action of MA with 200 ms depolarizing voltage steps at 30 s intervals was also examined (Fig. 1*B*). Steady-state inhibition was maintained for three successive voltage steps (90 s) prior to the subsequent perfusion of MA. As shown, the slowest inhibition time was 2·5 min with 10 pM and the fastest time to inhibition was obtained with 10 μM.

Short (50 ms) depolarizing voltage steps (Fig. 1*D*, inset) were acquired over the range of −80 to +70 mV to examine the current–voltage (I–V) relationship of the peak and tail currents, respectively. Between generation of the I–V traces, 200 ms depolarizing steps were acquired to assess control and steady-state values; thus the I–V value was

generated at steady-state values. Peak current was measured 5 ms prior to the end of the step. Figure 1*C* shows the *I–V* relationship of the high-threshold Ca^{2+} channel current averaged from three neurones. From a holding potential of −80 mV, the high-threshold current in VMN neurones is activated after −60 mV with a peak current amplitude at −10 mV, and an inflexion point between −40 and −20 mV. Perfusion with 1 μM MA inhibited the peak Ca^{2+} channel current, with an apparent voltage-dependent inhibition in the more negative voltage range (Fig. 1*C*, inset). For example, at −40 and +40 mV there was a 65 and 12% inhibition of the Ca^{2+} channel current, respectively.

The concentration–effect relationship for the steady-state inhibition of the peak Ca^{2+} channel current by MA was examined with 200 ms voltage steps to −10 mV from a holding potential of −80 mV. MA inhibited the Ca^{2+} channel current with a maximal inhibition of 24·4 ± 3·3%, an IC_{50} value of 2 nM and an n_H of 0·5, which suggested more than one binding site (Fig. 2). MA gave a maximal

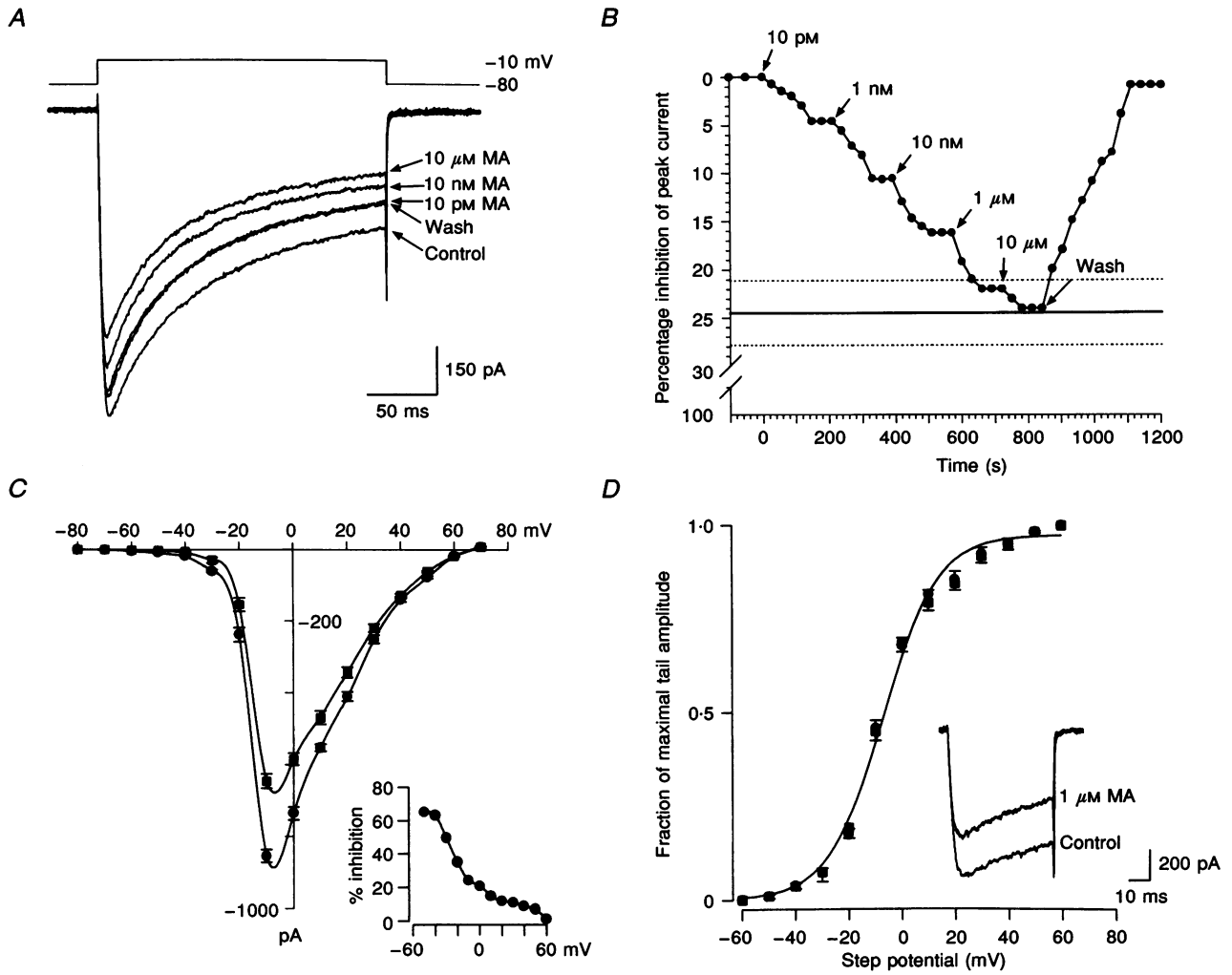

Figure 1. Megestrol acetate (MA) inhibition of whole-cell high-threshold Ca^{2+} channel currents in acutely isolated rat hypothalamic VMN neurones using 10 mM Ba^{2+} as the charge carrier

A, concentration-dependent inhibition of a fraction of the Ca^{2+} channel currents. Currents were elicited by 200 ms depolarizing voltage steps from a holding potential of −80 to −10 mV. Following a wash with control solution, the peak Ca^{2+} channel current returned to 92% of control. *B*, time course of the MA-induced inhibition in a different neurone. The continuous horizontal line represents the mean steady-state inhibition obtained with 10 μM MA (same data as control, Fig. 2); the dashed horizontal lines represent the S.E.M. *C*, mean current–voltage (*I–V*) relationship ($n = 3$). The Ca^{2+} channel current in these neurones peaked at −10 mV and there was no change in the shape of the *I–V* in presence of MA. Note the inflexion in the *I–V* curve between −40 and −20 mV. Inset shows the voltage-dependent inhibition by MA. Curves were fitted to a Boltzmann equation (see Methods). *D*, averaged tail current amplitudes at −80 mV from the neurones ($n = 3$) in *C* normalized to the maximum value (either control or MA, as appropriate). The half-maximal voltage for activation ($V_{½}$) and the slope factor (k) were −7·2 mV and 10·3. Inset shows an example of a 50 ms depolarizing step used to generate data in *C* and *D*.

inhibition of the Ca^{2+} channel current at saturating concentrations that inhibited only a fraction of the total Ca^{2+} channel current since a plateau effect was observed at 1 and 10 μM MA (23·5 ± 2·3 and 24·4 ± 3·3% inhibition, respectively). At this maximal concentration, there was little reversibility to 81 ± 4% of control with wash ($n = 9$), further suggesting that maximal inhibition had occurred. However, at lower concentrations such as 10 nM, there was good reversibility (94 ± 3% of control; $n = 9$).

We also examined some derivatives of MA. Medroxyprogesterone acetate showed an identical potency of inhibition to MA: 4 ± 1, 9 ± 4, 14 ± 3, 19 ± 3 and 23 ± 3% inhibition at 10 pM, 1 nM, 10 nM, 1 μM and 10 μM, respectively, with an IC_{50} of 4 nM and an n_H of 0·5 and with no reversibility (72 ± 4% of control) with wash following the 10 μM concentration ($n = 8$). Medroxyprogesterone weakly inhibited the peak Ca^{2+} channel current: 11 ± 2 and 15 ± 3% inhibition for 1 and 10 μM, respectively ($n = 4$). Progesterone had no effect on the peak Ca^{2+} current: 7 ± 1% inhibition at 10 μM ($n = 5$). To determine further whether MA acted at a binding site different from its parent compound, progesterone, we applied various concentrations of MA in the presence of 10 μM progesterone. There was no significant difference ($P > 0·4$) in the inhibition of the Ca^{2+} channel current by MA in the presence of progesterone compared with controls: 20 ± 1 and 21 ± 1% with 1 and 10 μM MA plus progesterone ($n = 5$) compared with 23·5 ± 2 and 24 ± 3% with 1 and 10 μM MA alone ($n = 10$ and 11, respectively).

In an attempt to distinguish between an external membrane receptor protein and/or channel protein site *versus* an intracellular site of action, we dialysed neurones with 10 nM MA added to the intracellular solution. This concentration was chosen as it was greater than the IC_{50} of 2 nM, and it was also the next concentration on the concentration–response curve. Following the normal run-up of the Ca^{2+} channel current, comparison of the MA-dialysed neurones ($n = 7$) with control neurones ($n = 13$) showed no significant difference ($P > 0·5$) in peak Ca^{2+} channel current amplitudes: 790 ± 23 and 819·7 pA for neurones dialysed with and without MA, respectively). Concomitant extracellular application of MA to MA-dialysed neurones did not cause a further significant depression ($n = 5$) in the peak Ca^{2+} channel current: 5 ± 1, 11 ± 2, 16 ± 2, 23·5 ± 2 and 24 ± 3% inhibition in control neurones (from Fig. 2) compared with 5 ± 2, 9 ± 2, 15 ± 2, 21 ± 3 and 23 ± 3% inhibition following external MA application with internal MA at 10 pM, 1 nM, 10 nM, 1 μM and 10 μM MA, respectively. Together, these data suggest, but do not conclusively prove, that MA interacts with its binding site from the external surface.

Activation and deactivation kinetics

The effect of MA on the voltage dependence of activation of the Ca^{2+} channel conductance was examined. Smooth curves to the peak tail current amplitudes (measured at −80 mV following a 50 ms depolarizing voltage step to various potentials) were fitted according to a Boltzmann distribution (see Methods). In three neurones examined with 1 μM MA, there was no change in the voltage at which half the channels are open ($V_{½}$) and the slope amplitude (k): $V_{½}$, −7·2 ± 0·5 and −7·1 ± 0·4 mV, and k, 10 ± 0·5 and 10·2 ± 0·4 mV for control and 1 μM MA, respectively. As there was no difference between control and 1 μM MA, the mean values ($n = 3$) are shown in Fig. 1*D*, where the fitted line gave a $V_{½}$ of −7·2 mV and a k of 10·3. Thus, MA had no effect on the voltage dependence of activation of the Ca^{2+} channel current.

To determine whether MA had an effect on the time course of deactivation of the Ca^{2+} currrent, we examined the time constants of the tail currents generated at −80 mV following a 50 ms depolarization step. The tail currents in these neurones were well fitted by a single exponential time constant (τ) (not shown). The deactivation of the Ca^{2+} channel current in VMN neurones is voltage dependent, with the speed of deactivation increasing as the repolarization level is brought to more negative levels: 188 ± 8, 211 ± 6, 248 ± 15, 286 ± 8, 355 ± 7, 402 ± 6, 408 ± 9, 434 ± 7, 460 ± 6 and 518 ± 7 μs for −40 to 50 mV (10 mV increments), respectively ($n = 3$). The tail currents in the inset to Fig. 1*D* had τ values of 290 and 320 μs and amplitudes of 947·4 and 631·6 pA, for control and 1 μM MA perfusates, respectively. Perfusion with 1 μM MA significantly ($P < 0·04$) slowed the deactivation of the tail currents uniformly over the same voltage range: 218 ± 6, 237 ± 5, 292 ± 4, 336 ± 13, 403 ± 6, 426 ± 6, 465 ± 6, 493 ± 7, 501 ± 8 and 596 ± 8 μs ($n = 3$).

To determine whether MA had an effect on the time course of activation, we examined whether the various concentrations of MA were slowing the time to peak of the inward Ca^{2+} channel current generated by the 200 ms depolarizing voltage steps. The activation or time to peak was fitted by a single exponential and was well described by a single time constant (τ) (not shown). Although there was an apparent slowing or increase in the time to peak of the Ca^{2+} channel current by MA, there was no significant difference ($P > 0·35$) in τ: 1·45 ± 0·12, 1·65 ± 0·2, 1·51 ± 0·17, 1·52 ± 0·22, 1·56 ± 0·14 and 1·55 ± 0·15 ms for control, 10 pM, 1 nM, 10 nM, 1 μM and 10 μM MA, respectively ($n = 6$).

Megestrol acetate and Ca^{2+} channel subtypes

As the pharmacology of the high-threshold Ca^{2+} channel current in VMN neurones was unknown, initial experiments were conducted to pharmacologically characterize these currents. Previous experiments in hippocampal neurones had found that a 10 μM concentration of CgTX was a maximal saturating concentration, and that a 10 μM nifedipine concentration was sufficient to block the L-type current (Mintz *et al.* 1992; ffrench-Mullen *et al.* 1994*a*). Increasing concentrations of Aga IVA blocked the peak Ca^{2+} channel

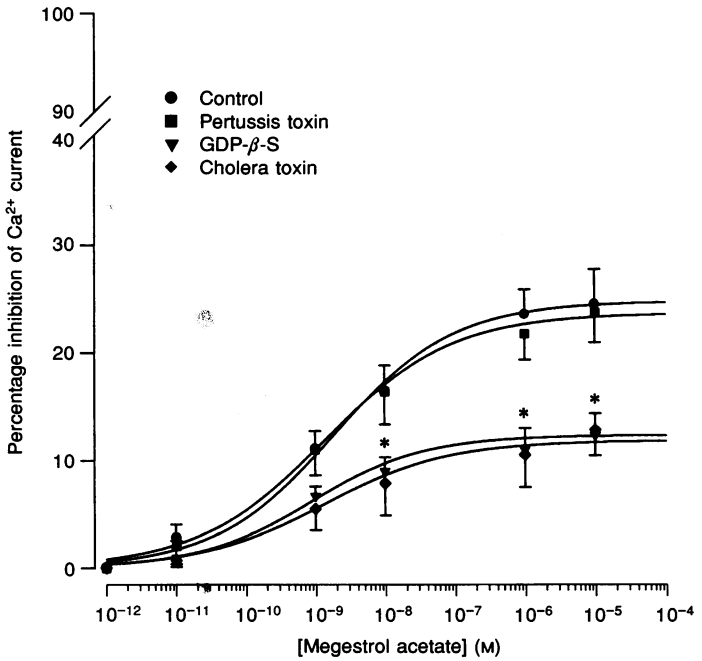

Figure 2. Concentration–effect curves for the MA-induced inhibition of the peak Ca^{2+} channel current

Ca^{2+} channel currents were evoked by 200 ms voltage steps from a holding potential of −80 to a test potential of −10 mV. Pertussis toxin had no effect on the MA-induced inhibition; in contrast, there was a significant difference (* $P < 0{\cdot}005$) between control and neurones treated with GDP-β-S and cholera toxin. Each point represents the mean ± S.E.M. of 8–12, 8–13, 5 and 8 neurones for control, pertussis toxin, GDP-β-S and cholera toxin, respectively.

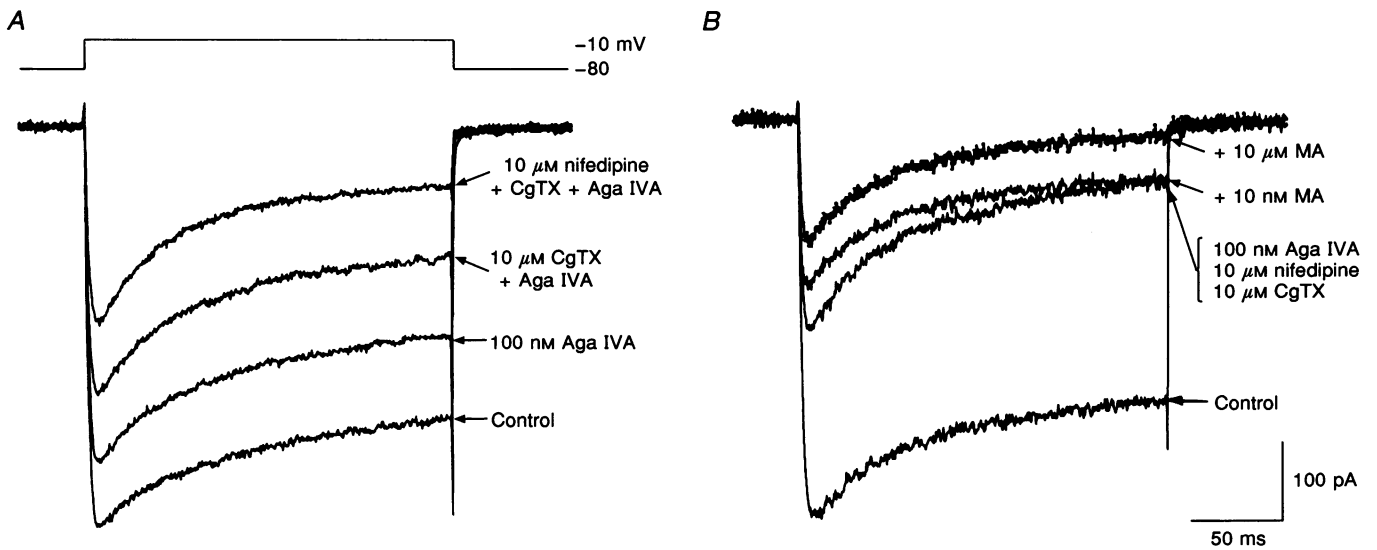

Figure 3. Pharmacology of the Ca^{2+} channel currents in rat VMN neurones

A, pharmacological identification of the various Ca^{2+} channel currents by subsequent perfusion with 100 nM ω-agatoxin IVA (Aga IVA; P-type), 10 μM ω-conotoxin GVIA (CgTX; N-type) and 10 μM nifedipine (nifedipine; L-type). A substantial fraction (37%) of the Ca^{2+} channel current, the residual current, remains uninhibited by these Ca^{2+} channel antagonists. *B*, following inhibition of the N-, L- and P-type Ca^{2+} channel currents (47% of peak current), perfusion with MA showed an additional 20% (10 nM MA) and 40% (10 μM MA) inhibition of the residual current.

current in a concentration-dependent manner: 0, 7 ± 2, 15 ± 3, 18 ± 3 and 17 ± 4% at 10, 100 pM, 1 nM, 10 nM and 100 nM, respectively, with an IC_{50} of 153 pM and an n_H of 1·1 ($n = 13$).

Figure 3*A* shows the typical effect of the sequential application of Aga IVA, CgTX and nifedipine on the Ca^{2+} channel current at −10 mV. In this neurone, 17% of the Ca^{2+} channel current was sensitive to Aga IVA, 19% to CgTX, and 28% to nifedipine; the residual current was 36% of the total current. When applied individually, 10 μM CgTX, 10 μM nifedipine and 100 nM Aga IVA blocked the Ca^{2+} channel current by 27·4 ± 4 ($n = 6$), 25 ± 3 ($n = 11$) and 17 ± 4% ($n = 6$), respectively, to give a total block of 69% (see Fig. 4*A–C*). Thus, we routinely used saturating concentrations of 10 μM CgTX and nifedipine, and 100 nM Aga IVA in our experiments

Sequential application of Aga IVA, CgTX and nifedipine (as illustrated in Fig. 3*A*) blocked the Ca^{2+} channel current by 16·3 ± 2, 20 ± 4 and 25 ± 3%, respectively, to give a total block of 61% ($n = 9$). Thus, in VMN neurones, a fraction of the high-threshold current (30–40%) remained, even in the presence of all three Ca^{2+} channel blockers. This residual current showed inactivation (Fig. 3*A*). Application of 100 nM Aga IVA following inhibition of the current by prior exposure to CgTX and/or nifedipine always gave 17 ± 3% inhibition ($n = 3$ each), indicating that Aga IVA always blocked the same fraction of Ca^{2+} channel current regardless of whether it was applied before or after CgTX and/or nifedipine. This is critical since there is non-additivity of block by CgTX and nifedipine, as it has previously been shown that the fraction of current blocked by the combination of CgTX and nifedipine is less than when the inhibitors are applied without prior exposure to each other (Regan *et al.* 1991). A similar situation occurred in VMN neurones with the combined application of CgTX, nifedipine and Aga IVA, since the fraction of current blocked was less (48 ± 3%; $n = 10$; Figs 3*B* and 4*D*) than the total block when the inhibitors were applied individually.

We first examined MA in the presence of 10 μM CgTX. Following the inhibition of the N-type current, increasing concentrations of MA continued to inhibit the Ca^{2+} channel current: 12 ± 2, 18 ± 2·5, 21 ± 2 and 27 ± 5% inhibition by 1 nM, 10 nM, 1 μM and 10 μM MA, respectively (Fig. 4*A*). In the presence of 10 μM nifedipine, levels of inhibition were 10 ± 2, 16 ± 4, 19 ± 3 and 24 ± 3% with 1 nM, 10 nM, 1 μM and 10 μM MA, respectively (Fig. 4*B*). Following 100 nM Aga IVA application, 10 ± 1, 16 ± 2, 21 ± 2 and 24 ± 3% inhibition of the current was induced by 1 nM, 10 nM, 1 μM and 10 μM MA, respectively (Fig. 4*C*). Thus, in the presence of these individual blockers, the MA inhibition was not different ($P > 0·5$) from control values (11 ± 2, 16 ± 3, 23·5 ± 3 and 24·5 ± 3% inhibition; see Fig. 2).

We next examined MA in the presence of CgTX, nifedipine and Aga IVA combined. The combined application of all three blockers inhibited the peak Ca^{2+} channel current by 47%; subsequent perfusion of MA in the presence of the three blockers inhibited the Ca^{2+} channel current by 22 and 40% for 10 nM and 10 μM MA, respectively (Fig. 3*B*). These results are summarized in Fig. 4*D*, where there was no significant difference ($P > 0·5$) in the Ca^{2+} channel current inhibition (9 ± 2, 16·5 ± 2, 22 ± 3 and 25 ± 4% for 1 nM, 10 nM, 1 and 10 μM MA, respectively) compared with control values (see above). Thus, MA partially inhibited the residual Ca^{2+} channel current.

G-protein mediation of the MA-induced inhibition

Experiments were next conducted to determine whether G-protein(s) were involved in modulation of the MA-induced inhibition. We first tested for a G-protein involvement in the MA-induced inhibition of Ca^{2+} channel current by internally dialysing the non-hydrolysable guanine nucleotide GDP-β-S (500 μM) through the recording electrode. By acting as a competitive inhibitor of GTP binding to the Gα-subunits, GDP-β-S inhibits the activation of Gα-subunits (Eckstein, Cassel, Levkovitz, Lowe & Selinger, 1979). GDP-β-S alone had no effect on the Ca^{2+} channel current peak amplitude (820 ± 26 pA for control, $n = 13$; 816 ± 34 pA for GDP-β-S, $n = 5$), and also time to peak (1·45 ± 0·12 ms for control, $n = 13$; 1·43 ± 0·07 ms for GDP-β-S; $n = 5$). GDP-β-S significantly diminished the MA-induced inhibition of the Ca^{2+} channel current at all concentrations except 10 pM and 1 nM ($P < 0·02$; maximum inhibition was 12 ± 3% at 10 μM) (Fig. 2), suggesting the involvement of a G-protein in the modulation of the MA-induced inhibition of the Ca^{2+} channel current.

To identify the subtype of G-protein mediating the MA response, we first examined the effects of pertussis toxin (PTX). Of the G-proteins expressed in neurones, some are sensitive to PTX (such as $G\alpha_i$ and $G\alpha_o$), which inactivates them by catalysing their ADP ribosylation (Helper & Gilman, 1992). Neurones were acutely isolated from animals pretreated for 48 h with PTX (1000 ng (24 h)$^{-1}$ for 48 h). PTX had no effect on the peak Ca^{2+} current amplitude (820 ± 26pA for control, $n = 13$; 817 ± 23 pA for PTX, $n = 10$) and time to peak (1·45 ± 0·12 ms for control; $n = 13$; 1·5 ± 0·07 ms for PTX; $n = 6$). As illustrated in Fig. 2, PTX had no effect on the MA-induced inhibition of the Ca^{2+} channel current, which suggested a lack of involvement of $G\alpha_i$- and $G\alpha_o$-subunits.

We next examined neurones from animals treated with cholera toxin (CTX) (100 ng (24 h)$^{-1}$ for 48 h), which irreversibly activates, via ADP ribosylation, an internal arginine residue in the $G\alpha_S$-subunit (Helper & Gilman, 1992). At this concentration of CTX, no significant behavioural effects on measured daily food and water

intake were observed ($n = 7$ rats). CTX had no effect on the characteristics of the Ca^{2+} channel current such as peak amplitude (820 ± 26 and 817 ± 28 pA) and time to peak (1·45 ± 0·12 and 1·44 ± 0·06 ms) for control ($n = 13$) and CTX ($n = 8$), respectively. An example of the effect of CTX on the MA-induced inhibition of the Ca^{2+} channel current is illustrated in Fig. 5*A*, where peak current inhibition by 10 μM MA was 10%. CTX significantly diminished the MA-induced inhibition at all concentrations examined except 10 pM and 1 nM ($P < 0·015$; maximum inhibition was 12·8 ± 3% at 10 μM) (Fig. 2).

To verify further the $G\alpha_S$-subunit involvement in the MA-induced inhibition of the Ca^{2+} channel current, we used specific antisense phosphothio-oligodeoxynucleotides. Animals were treated with 15 μg $(24\ h)^{-1}$ for 48 h of antisense or sense to the $G\alpha_S$-subunit and antisense to the $G\alpha_{11}$-subunit. These treatments also had no effect on measured food and water intake ($n = 11$ rats). The oligodeoxynucleotides had no effect on the Ca^{2+} channel current, such as peak amplitude (820 ± 26 pA for control, $n = 13$; 821 ± 16 pA for antisense-$G\alpha_S$, $n = 9$; 816 ± 9 pA for sense-$G\alpha_S$; $n = 6$; 818 ± 27 pA for antisense-$G\alpha_{11}$, $n = 4$) and time to peak (1·45 ± 0·12 ms for control, $n = 13$; 1·54 ± 0·06 ms for antisense-$G\alpha_S$, $n = 9$; 1·48 ± 0·07 ms for sense-$G\alpha_S$, $n = 6$; 1·5 ± 0·1 ms for antisense-$G\alpha_{11}$, $n = 3$).

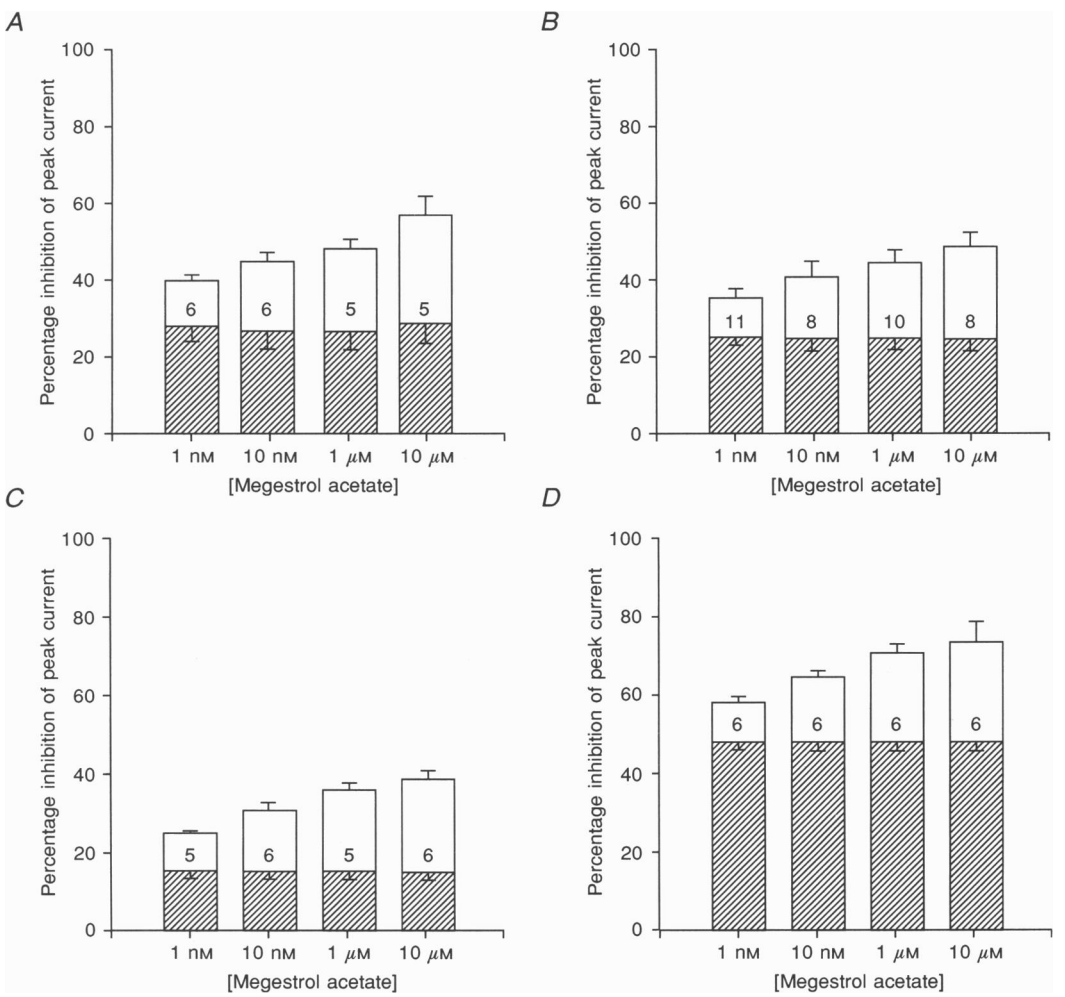

Figure 4. Summary of the MA-induced inhibition of the residual Ca^{2+} channel current

Data were taken from the peak Ca^{2+} channel current evoked by 200 ms voltage steps from a holding potential of −80 mV to a test potential of −10 mV. *A*, in the presence of 10 μM CgTX (inhibition of the N-type Ca^{2+} channel current; ▨), MA inhibited an additional fraction but not all the remaining current (□). *B*, in the presence of 10 μM nifedipine (inhibition of the L-type Ca^{2+} channel current; ▨), MA continued to inhibit a fraction of the remaining current. *C*, in the presence of 100 nM Aga IVA (inhibition of the P-type Ca^{2+} channel current; ▨), MA continued to inhibit a fraction of the remaining Ca^{2+} channel current. *D*, in the presence of CgTX, nifedipine and Aga IVA (inhibition of the N-, L- and P-type Ca^{2+} channel currents; ▨) MA continued to inhibit a fraction of the remaining Ca^{2+} channel current. Data are expressed as means ± S.E.M.; number of neurones examined is given in each column.

The diminution of the MA-induced effect by antisense-Gα_S is illustrated in Fig. 5*B*, where there was a maximum of 9% inhibition by 10 μM MA. In contrast, the inhibition of the Ca^{2+} channel current induced by 10 μM MA was 20% in the presence of sense-Gα_S (Fig. 5*C*). The antisense-Gα_{11} had no effect on the MA-induced inhibition: 5 ± 1, 10 ± 1, 14 ± 2, 21 ± 3 and 22 ± 2% inhibition at 10 pM, 1 nM, 10 nM, 1 μM and 10 μM MA, respectively ($n = 4$). Similarily, the sense-Gα_S also had no significant effect on the MA-induced inhibition: $3{\cdot}7 \pm 0$, $9{\cdot}5 \pm 1$, $13{\cdot}6 \pm 1$, $20{\cdot}2 \pm 2$ and $21{\cdot}3 \pm 1$% inhibition at 10 pM, 1 nM, 10 nM, 1 μM and 10 μM MA, respectively (Fig. 5*D*). In contrast, the antisense-Gα_S significantly ($P < 0{\cdot}004$) diminished the MA-induced inhibition of the Ca^{2+} channel current at all concentrations except 10 pM: 2 ± 0, 4 ± 1, $5{\cdot}5 \pm 1$, $6{\cdot}8 \pm 2$ and 9 ± 2% at 10 pM, 1 nM, 10 nM, 1 μM and

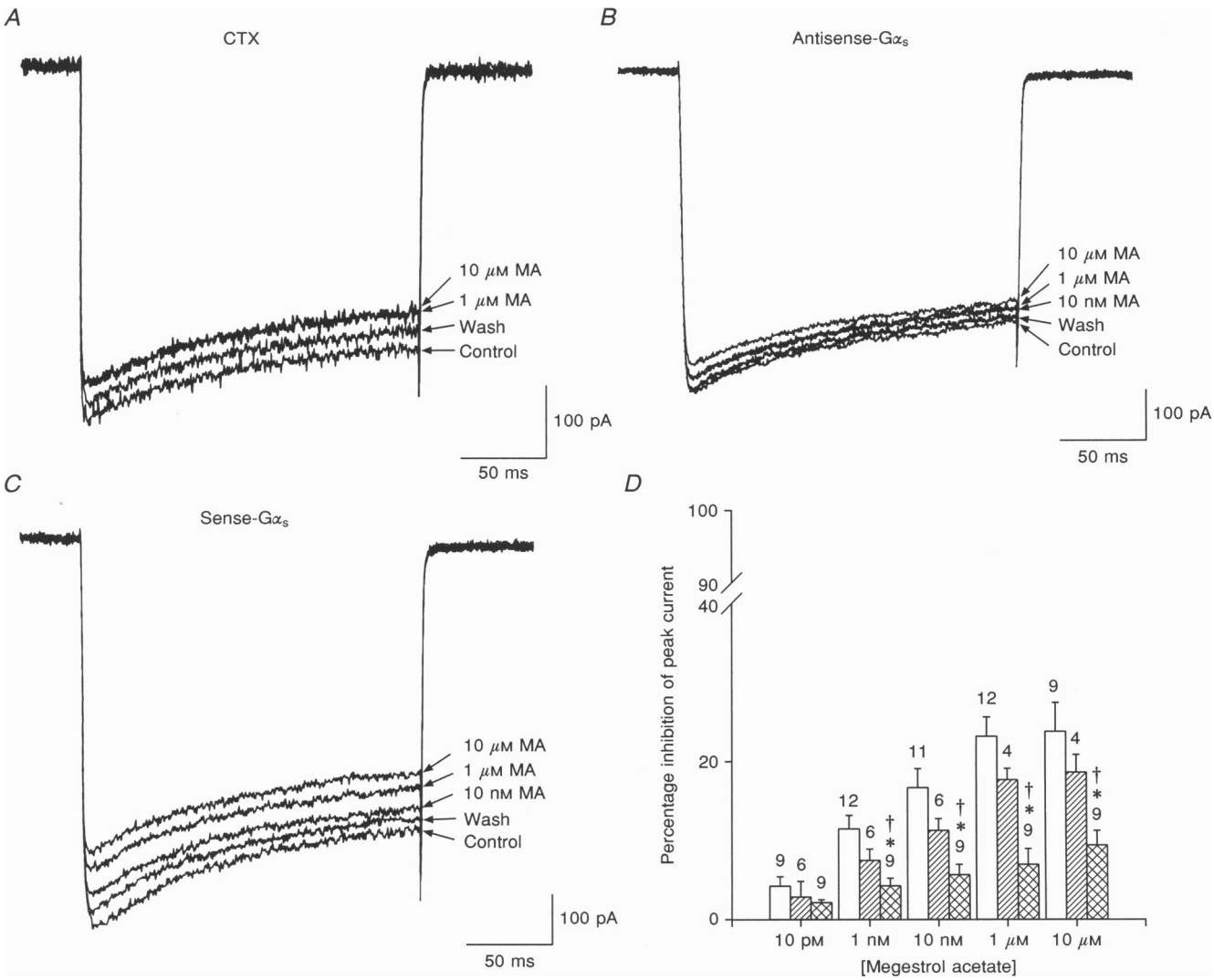

Figure 5. The G-protein α_S-subunit modulates the MA-induced inhibition of the residual Ca^{2+} channel current

A, MA (10 μM) had a minimal inhibitory effect (10%) in VMN neurones obtained from cholera toxin (CTX)-treated animals (100 ng (24 h^{-1}) for 48 h) compared with control ($24{\cdot}5 \pm 3{\cdot}3$%); this suggested a CTX-sensitive G-protein involvement. *B*, treatment with the phosphothio-oligodeoxynucleotide, antisense-Gα_S (15 μg (24 h^{-1}) for 48 h) diminished the 10 μM MA-induced inhibition to 9%. *C*, treatment with sense-Gα_S (15 μg (24 h^{-1}) for 48 h) had no effect on the 10 μM MA-induced inhibition (20%) compared with control. *D*, summary of the effects of the phosphothio-oligonucleotide treatment on the MA-induced inhibition of the Ca^{2+} channel current. Control values (□) are taken from Fig. 2; number of neurones examined is given above each column. There was no significant difference in the inhibition between control and sense-Gα_S (▨). There were significant differences between control and antisense-Gα_S (▩) (* $P < 0{\cdot}004$), and between the antisense-Gα_S and the sense-Gα_S († $P < 0{\cdot}003$). Neurones were acutely isolated from animals treated with cholera toxin and the various phosphothio-oligodeoxynucleotides (see Methods for details).

10 μM MA, respectively (Fig. 5*D*). Comparison of the antisense to the sense oligodeoxynucleotide also showed a significant ($P < 0{\cdot}003$) reduction of the MA-induced inhibition of the Ca^{2+} channel current. In contrast, there was no significant difference between the sense-Gα_S and control.

The specificity of the antisense-Gα_S for MA-induced inhibition of the Ca^{2+} channel current is suggested because the sense-Gα_S and the antisense-Gα_{11} had no effect. Furthermore, the stability of the antisense-treated neurones was confirmed by the lack of effect on either the amplitude or time to peak of the Ca^{2+} channel currents.

Involvement of PKC and PKA in the MA-induced inhibition

These experiments led to the conclusion that the MA-induced inhibition of the residual Ca^{2+} channel current was mediated via a G-protein-coupled mechanism, specifically the α_S-subunit. The modulation of Ca^{2+} channels by G-protein-coupled receptors involves a variety of mechanisms, including a direct action of the activated α-subunit and/or intracellular mediators (for review, see Hille, 1992).

To determine whether the MA-induced activation of the Gα_S-subunit and its coupling to Ca^{2+} channels involved intracellular mediators such as protein kinase C (PKC) and protein kinase A (PKA), we examined the effects of specific inhibitors of PKC and PKA. The specific inhibitor of PKC, synthetic pseudosubstrate inhibitor PKCI(19–36) (House & Kemp, 1987), is believed to be effective against all forms of PKC (Bell & Burns, 1991; Orr, Keranen & Newton, 1992). Bisindolylmaleimide (BIS) is a potent and highly selective inhibitor of PKC (Toullec *et al.* 1991). The characteristics of neurones internally dialysed with BIS and PKCI(19–31) were the same as those not dialysed with these compounds, as previously reported (ffrench-Mullen *et al.* 1994*a*). Following the normal run-up of the Ca^{2+} channel current, PKCI(19–31) and BIS had no effect on the amplitude and the time to peak of the Ca^{2+} channel current (not shown; $n = 3$, respectively).

Figure 6*A* summarizes the results of internal dialysis (through the patch pipette) of both PKCI(19–31) (1 μM) and BIS (2 μM); there was a significant diminution ($P < 0{\cdot}01$, for both inhibitors) of the MA-induced inhibition of the Ca^{2+} channel current at all concentrations. The maximal MA-induced inhibition at 10 μM was 14 ± 3% for PKCI(19–31) and 11 ± 3% for BIS.

To determine whether there was a cAMP-dependent protein kinase (PKA) involvement, we tested the 20 amino acid (20 AA) protein kinase inhibitor (internal dialysis through

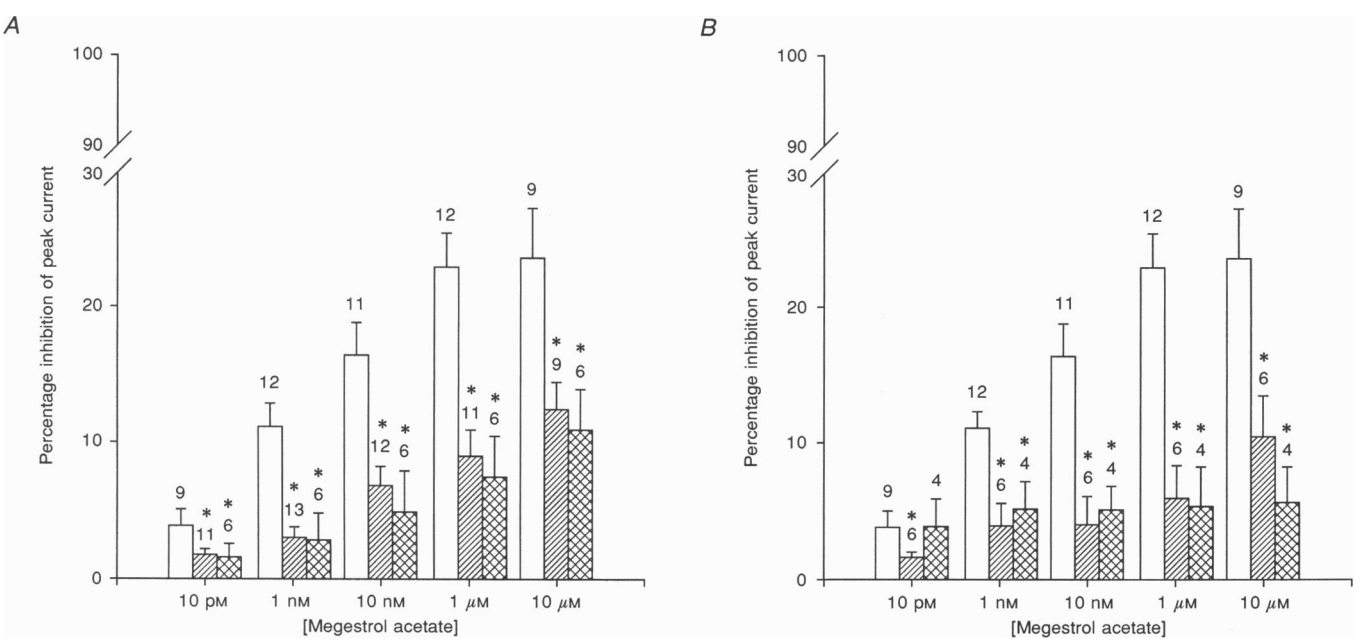

Figure 6. MA-induced inhibition of the Ca^{2+} channel current involves activation of PKC and PKA

The specific PKC inhibitors bisindolylmaleimide (BIS) and the pseudosubstrate inhibitor PKCI(19–36) and the 20 amino acid (20 AA) PKA inhibitor were internally dialysed through the patch pipette. The specific PKA inhibitor, Rp-cyclic adenosine 3′,5′-monophosphothioate (Rp-cAMPS), was applied extracellulary. Control data (□) are taken from Fig. 2. *A*, BIS (2 μM; ▨) and PKCI(19–36) (1 μM; ▩) significantly reduced (* $P < 0{\cdot}01$) the MA-induced inhibition of the Ca^{2+} channel current. *B*, 20 AA (2 μM; ▨), Rp-cAMPS (100 μM; ▩) significantly reduced (* $P < 0{\cdot}01$) the MA-induced inhibition of the Ca^{2+} channel current.

the patch pipette) which inhibits the phosphorylating units of cAMP-dependent kinase in skeletal muscle (Cheng *et al.* 1986). As shown in Fig. 6*B*, this 20 AA (2 μM) inhibitor significantly ($P < 0.01$) diminished the MA-induced inhibition of the Ca^{2+} channel current, with the maximal inhibition of $11 \pm 3\%$ at 10 μM MA. Rp-cAMPS, a competitive inhibitor of PKA which competes with cAMP for the binding site on the regulatory subunit of PKA was also examined (Dostman, Taylor, Genieser, Jasteroft, Doskeland & Ogried, 1990; Frey, Huang & Kandel, 1993). Extracellular application of 100 μM Rp-cAMPS also significantly ($P < 0.01$) diminished the MA-induced inhibition of the residual Ca^{2+} channel current (Fig. 6*B*).

These results suggest that both PKC and PKA are involved with the MA-induced inhibition of the Ca^{2+} channel current. To test this hypothesis further, we combined both BIS (2 μM) and the 20 AA (2 μM) inhibitors in the patch pipette. Internal dialysis of both inhibitors significantly ($P < 0.002$) eliminated the MA-induced inhibition: 0, 0, 1.8 ± 2, 2.4 ± 2 and $5 \pm 3\%$ inhibition for 10 pM, 1 nM, 10 nM, 1 μM and 10 μM MA, respectively ($n = 5$). This combination was essentially additive since there was no effect at the lower concentrations of MA, and at 10 μM, the combination inhibition was half that observed with the individual inhibitors (11%). These results further suggest that both PKC and PKA are involved with the MA-induced inhibition of the Ca^{2+} channel current.

DISCUSSION

The results of this study document for the first time an action of megestrol acetate in the central nervous system, specifically at the VMN, which is involved in the integrative regulation of satiety mechanisms. One of MA's primary clinical uses is to induce weight gain in cachectic/anorectic patients.

Inhibition of the Ca^{2+} channel current by MA

While MA had no effect on the low-threshold or T-type Ca^{2+} channel current, it potently inhibited a fraction of the high-threshold whole-cell Ca^{2+} channel current in VMN neurones with an IC_{50} of 2 nM and a Hill coefficient of 0.5, which suggested more than one binding site.

The MA analogue medroxyprogesterone acetate showed an equal potency of inhibition of the Ca^{2+} channel current, suggesting a similar site of action to MA. This compound is identical to MA with the exception of the lack of a double bond between carbons 6 and 7. Medroxyprogesterone, which lacks the acetate but retains the methyl group on carbon 6, was a weaker inhibitor of the Ca^{2+} channel current than either MA or medroxyprogesterone acetate, thus suggesting an acetate requirement. Progesterone, the 'parent compound', had no effect on the peak Ca^{2+} channel current in these neurones; similar observations were reported for hippocampal CA1 neurones (ffrench-Mullen *et al.* 1994*a*). In contrast, progesterone is known to affect ligand-gated currents, for example by enhancing GABA-induced responses in Purkinje and spinal chord neurones (Smith, Waterhouse & Woodward, 1987; Wu, Gibbs & Farb, 1990) and inhibiting the nicotinic ACh response (Bertrand, Valera, Bertrand, Ballivet & Rungger, 1991). In the presence of 10 μM progesterone, there was no difference in the amount of inhibition by MA of the Ca^{2+} channel current compared with that induced by 10 μM MA alone. The data suggest that MA binds to an extracellular receptor site on the cell membrane surface or a site within the lipid–protein interface. If MA depressed the Ca^{2+} channel current by perturbing the membrane structure or by binding to a hydrophobic region of the Ca^{2+} channel bound to a membrane lipid, then internally dialysed MA would have strongly reduced the run-up of the Ca^{2+} channel current. Additionally, intracellular MA would dramatically reduce the effect of extracellularly applied MA. The lack of effect of internally dialysed MA on the Ca^{2+} channel current and the fact that the combination of extracellularly applied and internally dialysed MA showed a comparable inhibition suggests that MA can only access its binding site from the extracellular surface. Similar observations concerning neuroactive steroids on Ca^{2+} channel currents in hippocampal CA1 neurones (ffrench-Mullen *et al.* 1994*a*) and the $GABA_A$ inward current (Lambert, Hill-Vining, Peters, Sturgess & Hales, 1991) have been reported.

The modulation of Ca^{2+} channel currents in numerous neuronal cell types is known to change both the time course and voltage dependence of Ca^{2+} currents (Carbonne & Swandulla, 1989). There was no change in the shape of the I–V relationship following application of MA although maximal inhibition of the peak inward current occurred at more negative step potentials. MA had no effect on the voltage-dependent activation of the Ca^{2+} channel current. However, there was a slowing of channel kinetics as shown by the increase in deactivation of the Ca^{2+} channel current.

Pharmacological characterization of MA-induced inhibition

As with other central neurones, the high-threshold Ca^{2+} channel current in VMN neurones can be pharmacologically characterized into the CgTX-sensitive (N-type) current, the nifedipine-sensitive (L-type) current, the Aga IVA-sensitive (P-type) current and a current insensitive to these antagonists, the residual current. None of these antagonists had any effect on the MA-induced inhibition of the Ca^{2+} channel current; MA specifically inhibited approximately 50% of the residual Ca^{2+} channel current. The balance of the residual current in these neurones could be carried by T-type channels, as it has recently been shown that part of the resistant current is carried by T-type channels (Eliot & Johnston, 1994; Unemiya & Berger, 1994).

MA-induced inhibition occurs through a novel signal transduction pathway

Unlike the action of other neuroactive steroids that utilize a PTX-sensitive G-protein to modulate Ca^{2+} channels in mammalian hippocampal neurones (ffrench-Mullen *et al.* 1994*a*), the MA-induced inhibition of the residual Ca^{2+} channels resulted from activation of a CTX-sensitive G-protein. CTX is known to ADP-ribosylate the α-subunit of G_S, G_{olf} and transducin (Helper & Gilman, 1992). Treatment with antisense-$G\alpha_S$ significantly diminished the MA-induced inhibition of the residual Ca^{2+} channel current; in contrast, the sense-$G\alpha_S$, and antisense-$G\alpha_{11}$, which attenuates the cholinergic inhibition of the delayed rectifier potassium current in VMN neurones (ffrench-Mullen *et al.* 1994*a*) had no effect. Together, these results verified the identity of the G-protein α_S-subunit modulating the MA-induced inhibition of the residual Ca^{2+} channel current in these neurones.

As ADP ribosylation by CTX is believed to inhibit the intrinsic GTPase activity of the $G\alpha_S$-subunit, resulting in persistent activation (Cassel & Selinger, 1977), CTX treatment usually mimics the results of activation of various receptors coupled to the $G\alpha_S$-subunit. Thus, one might anticipate that CTX would mimic the effects of MA and inhibit the Ca^{2+} channel current. However, CTX treatment did not mimic the MA response as there were no differences in the electrophysiological characteristics (amplitude and time to peak) of the Ca^{2+} channel current following CTX application compared with controls. A similar observation was found regarding the VIP-mediated inhibition of Ca^{2+} channels via CTX in mammalian sympathetic neurones (Zhu & Ikeda, 1994). As with MA, the VIP inhibition of the Ca^{2+} channels was not mimicked by CTX, and there were no changes in the current characteristics. Indeed, there are a few similar cases reported in the literature (see Zhu & Ikeda, 1994). Thus, our data are similar to those of Zhu & Ikeda (1994), suggesting a different coupling mechanism between the $G\alpha_S$-subunit and its effectors.

The $G\alpha_S$-subunit is coupled to adenylate cyclase which leads to cAMP production and subsequent PKA activation. The $G\alpha_S$-dependent MA-induced inhibition of the residual Ca^{2+} channel current is coupled to PKA since specific inhibitors of PKA significantly diminished the MA-induced inhibition. This is in contrast to the CTX-modulated VIP-induced inhibition of Ca^{2+} channels which was membrane delimited and thus independent of cAMP or PKA (Zhu & Ikeda, 1994). Furthermore, specific inhibitors of PKC also diminished the MA-induced inhibition of the residual Ca^{2+} current, and the combination of both inhibitors of PKC and PKA in the recording electrode led to an even greater reduction of the MA response. The results therefore show that PKA and PKC are involved in the MA-induced inhibition of the residual Ca^{2+} channel current in VMN neurones.

Physiological and pharmacological significance

Megestrol acetate is a progesterone derivative commonly used for the treatment of metastatic breast and endometrial cancer, but is now seeing prominent usage to increase appetite, and hence weight gain, in cachectic/anorectic patients. While MA causes appetite stimulation and weight gain with minimal side effects, the precise mechanism(s) of action is unknown.

The results of this study suggest a novel, extracellular steroid receptor site, and a specificity of action of MA in the VMN. This is further clarified by the lack of effect of progesterone on the Ca^{2+} channel current and on the MA-induced inhibition as there are progesterone receptors in the VMN involved in female sexual behaviour (see Richmond & Clemens, 1988). The MA-induced inhibition is mediated via an G-protein α_S-subunit and intracellular kinases, suggesting a discrete modulation of neuronal firing. It has been suggested that weight gain due to MA is dependent upon anabolic effects and the accumulation of intracellular lipids (Hamburger, Parnes, Gordon, Shantz, O'Donnell & Aisner, 1988). However, our results suggest that the appetite-stimulating effect of MA may, in part, be due to its action at the VMN. The VMN is known to participate in the integrative regulation of satiety mechanisms (see Plata-Salamán, 1991), where stimulation of the VMN, and hence cell firing, inhibits food intake (Bielajew *et al.* 1994). The MA-induced inhibition of the residual Ca^{2+} channel current would attenuate neuronal firing of VMN neurones. This would result in increased food intake.

Aisner, J., Tchekmedyian, N. S., Moody, M. & Tait, N. (1987). High-dose megestrol acetate for treatment of advanced breast cancer. *Seminars in Hematology* **24**, 48–55.

Akaike, N., Kostyuk, P. G. & Osipchuk, Y. V. (1989). Dihydropyridine-sensitive low-threshold calcium channels in isolated rat hypothalamic neurones. *Journal of Physiology* **412**, 181–195.

Bell, R. & Burns, D. (1991). Lipid activation of protein kinase C. *Journal of Biochemistry* **266**, 4661–4664.

Bertrand, D., Valera, S., Bertrand, S., Ballivet, M. & Rungger, D. (1991). Steroids inhibit nicotinic acetylcholine receptors. *NeuroReport* **2**, 277–280.

Bielajew, C., Stenger, J. & Schindler, D. (1994). Factors contributing to the reduced weight gain following chronic ventromedial hypothalamic stimulation. *Behavioural Brain Research* **62**, 143–148.

Bruera, E. (1992). Current pharmacological management of anorexia in cancer patients. *Oncology* **6**, 125–130.

Carbonne, E. & Swandulla, D. (1989). Neuronal calcium currents: kinetics, blockade and modulation. *Progress in Biophysics and Molecular Biology* **54**, 31–58.

Cassel, D. & Selinger, Z. (1977). Mechanism of adenlyate cyclase activation by cholera toxin: inhibition of GTP hydrolysis at the regulatory site. *Proceedings of the National Academy of Sciences of the USA* **74**, 3307–3311.

CHENG, H. C., KEMP, B. E., PEARSON, R. B., SMITH, A. J., MISCONI, L., VAN PATTEN, S. M. & WALSH, D. A. (1986). A potent synthetic peptide inhibitor of the cAMP-dependent protein kinase. *Journal of Biological Chemistry* **261**, 989–992.

DOSTMANN, W. R. G., TAYLOR, S. S., GENIESER, H.-H., JASTEROFF, B., DOSKELAND, S. O. & OGRIED, D. (1990). Probing the nucleotide binding sites of cAMP-dependent protein kinases I and II with analogs of adenosine 3′,5′-cyclic phosphorothioates. *Journal of Biological Chemistry* **265**, 10484–10491.

ECKSTEIN, F., CASSEL, D., LEVKOVITZ, H., LOWE, M. & SELINGER, Z. (1979). Guanosine 5′-*O*-(2-thiodiphosphate). An inhibitor of adenylate cyclase stimulation by guanine nucleotides and fluoride ions. *Journal of Biological Chemistry* **254**, 9829–9834.

ELIOT, L. S. & JOHNSTON, D. (1994). Multiple components of calcium current in acutely dissociated dentate gyrus granule neurons. *Journal of Neurophysiology* **72**, 762–777.

FFRENCH-MULLEN, J. M. H., DANKS, P. & SPENCE, K. T. (1994*a*). Neurosteroids modulate calcium currents in hippocampal CA1 neurons via a pertussis toxin-sensitive G-protein-coupled mechanism. *Journal of Neuroscience* **14**, 1963–1977.

FFRENCH-MULLEN, J. M. H., PLATA-SALAMÁN, C. R., BUCKLEY, N. J. & DANKS, P. (1994*b*). Muscarinic modulation by a G-protein α-subunit of delayed rectifier K^+ current in rat ventromedial hypothalamic neurones. *Journal of Physiology* **471**, 21–26.

FREY, U., HUANG, Y.-Y. & KANDEL, E. R. (1993). Effects of cAMP stimulate a late stage of LTP in hippocampal neurons. *Science* **260**, 1661–1664.

GRAHAM, K. K., MIKOLICH, D. J., FISHER, A. E., POSNER, M. R. & DUDLEY, M. N. (1994). Pharmacologic evaluation of megestrol acetate oral suspension in cachetic AIDS patients. *Journal of Acquired Immune Deficiency Syndromes* **7**, 580–586.

GREGORY, E. J., COHEN, S. C., OINES, D. W. & MIMS, C. H. (1985). Megestrol acetate therapy for advanced breast cancer. *Journal of Clinical Oncology* **3**, 155–160.

HAMBURGER, A. W., PARNES, H., GORDON, G. B., SHANTZ, L. M., O'DONNELL, K. A. & AISNER, J. (1988). Megestrol acetate-induced differentiation of 3T3-L1 adipocytes *in vitro*. *Seminars in Oncology* **15**, supplement 1, 76–78.

HELPER, J. R. & GILMAN, A. G. (1992). G-proteins. *Trends in Biochemical Sciences* **17**, 383–387.

HILLE, B. (1992). G-protein coupling mechanisms and nervous system signalling. *Neuron* **9**, 187–195.

HOUSE, C. & KEMP, B. E. (1987). Protein kinase C contains a pseudosubstrate prototype in its regulatory domain. *Science* **238**, 1726–1728.

LAMBERT, J. J., HILL-VINING, C., PETERS, J. A., STURGESS, N. C. & HALES, T. G. (1991). The actions of the anaesthetic steroids on inhibitory and excitatory receptors. In *FIDIA RF Symposium Series*, vol. 6, ed. COSTA, E. & BARNARD, E., pp. 219–236. Thieme, New York.

LOPRINZI, C. L., GOLDBERG, R. M. & BURNHAM, N. L. (1992). Cancer-associated anorexia and cachexia. Implications for drug therapy. *Drugs* **43**, 499–506.

LOPRINZI, C. L., SCHAID, D. J., DOSE, A. M., BURNHAM, N. L. & JENSEN, M. D. (1993). Body-composition changes in patients who gain weight while receiving megestrol acetate. *Journal of Clinical Oncology* **11**, 152–154.

MINTZ, I. A., ADAMS, M. E. & BEAN, B. P. (1992). P type calcium channels in rat central and peripheral neurons. *Neuron* **9**, 85–95.

MORGAN, L. R. (1985). Megestrol acetate *vs.* tamoxifen in advanced breast cancer in postmenopausal patients. *Seminars in Oncology* **12**, 43–47.

NELSON, K. A., WALSH, D. & SHEEHAN, F. A. (1994). The cancer anorexia-cachexia syndrome. *Journal of Clinical Oncology* **12**, 213–225.

ORR, J., KERANEN, L. & NEWTON, A. (1992). Reversible exposure of the pseudosubstrate domain of protein kinase C by phosphatidylserine and diacylglycerol. *Journal of Biological Chemistry* **267**, 15263–15266.

PLATA-SALAMÁN, C. R. (1991). Regulation of hunger and satiety in man. *Digestive Diseases* **9**, 253–268.

REGAN, L. J., SAH, D. W. Y. & BEAN, B. P. (1991). Ca^{2+} channels in rat central and peripheral neurons: high-threshold current resistant to dihydropyridine blockers and ω-conotoxin. *Neuron* **6**, 269–280.

RICHMOND, G. & CLEMENS, L. (1988). Ventromedial hypothalamic lesions and cholinergic control of female sexual behaviour. *Physiology and Behaviour* **42**, 179–182.

SMITH, S. S., WATERHOUSE, B. D. & WOODWARD, D. J. (1987). Locally applied progesterone metabolites alter neuronal responsiveness in the cerebellum. *Brain Research Bulletin* **18**, 739–747.

TISDALE, M. J. (1993). Cancer cachexia. *Anti-cancer Drugs* **4**, 115–125.

TOULLEC, D., PIANETTI, P., COSTE, H., BELLENVERGUE, P., GRAND-PERRET, T., AJAKANES, M., BAUDET, V., BOISSIN, P., BOURSIER, E., LORIOLLE, F., DUHAMEL, L., CHARON, D. & KIRILOVSKY, J. (1991). The bisindolylmaleimide GF 109203X is a potent and selective inhibitor of protein kinase C. *Journal of Biological Chemistry* **266**, 15771–15781.

TSIEN, R. W., LIPSCOMBE, D., MADISON, D. V., BLEY, K. R. & FOX, A. P. (1988). Multiple types of calcium channels and their selective modulation. *Trends in the Neurosciences* **11**, 431–438.

UNEMIYA, M. & BERGER, A. J. (1994). Properties and function of low- and high-voltage-activated Ca^{2+} channels in hypoglossal neurons. *Journal of Neuroscience* **14**, 5652–5660.

WANG, H.-Y., WATKINS, D. C. & MALBON, C. C. (1992). Antisense oligodeoxynucleotides to G_S protein α-subunit sequence accelerate differentiation of fibroblasts to adipocytes. *Nature* **358**, 334–337.

WU, F.-S., GIBBS, T. T. & FARB, D. H. (1990). Inverse modulation of gamma-aminobutyric acid- and glycine-induced currents by progesterone. *Molecular Pharmacology* **37**, 597–602.

ZHU, Y. & IKEDA, S. R. (1994). VIP inhibits N-type Ca^{2+} channels of sympathetic neurons via a pertussis toxin-insensitive but cholera toxin-sensitive pathway. *Nature* **13**, 657–669.

Received 31 October 1994; accepted 9 February 1995.